Supplemental Figure 1: Distribution of GFP::GBDwsp-1 fluorescent lifetimes in embryos expressing either GFP::GBDwsp-1 alone or co-expressed with either mCHERRY::CDC-42(T17N) or mCHERRY::CDC-42(Q61L)

The fluorescence lifetime of GFP::GBDwsp-1 (expressed from one genetic copy; GFP-only cross products) was statistically indistinguishable in embryos expressing GFP::GBDwsp-1 alone (GFP only cross products) vs coexpressed with mCHERRY::CDC-42(T17N) (WH432xWH517, $p>0.8$), but was significantly shortened when coexpressed with CDC-42(Q61L) (WH423xWH517, $p<0.01$) and was significantly lengthened when expressed from 2x genetic dose (WH517 GFP only, $p<0.02$).

Supplemental Figure 2: Localization of GFP-tagged CDC-42 and two of its mutant forms

Timeseries of the localization of GFP-fusions of CDC-42, the constitutively inactive mutant T17N and the constitutively active mutant Q61L in embryos from polarization to 2-cell stage. Arrowheads indicate polarized enrichment of cortical signal. Scale bar is 10μm.

Supplemental Figure 3: Localization of GFP-tagged CGEF-1A
Timeseries of the localization of a GFP-fused CGEF-1A. There is enrichment of the nucleoplasm and a subtle enrichment at the cortex in Phase II. Scale bar is 10μm.

Supplemental Figure 4: Observed maximum speeds of GFP::NMY-2-labeled cortical regions during Phase I

The flow rates of five of the fastest moving GFP::NMY-2 puncta were measured from kymographs of timeseries collected from embryos of the described genotype. Error bars represent the observed SEM and are absent in conditions with a single usable embryo. "*" indicates that the measured speeds were statistically significantly different from those of the wild type at $p<0.05$.

Supplemental Figure 5: RHO-1 and CDC-42 pathway components are required to recruit GFP::NMY-2 to the cortex in distinct phases

Embryos expressing GFP::NMY-2 in the early embryo. In the wild type, GFP::NMY-2 localizes to the cortex in distinct morphological distributions in Phases I and II. The robust myosin foci observed in Phase I depend upon ECT-2, RHO-1 and LET-502. The robust, diffuse, polar distribution of smaller myosin puncta in Phase II depends upon CGEF-1, CDC-42 and MRCK-1. Disruption of either pathway does not abolish the recruitment by the other, and disruption of both pathways disrupts both recruitment patterns. Double disruptions tested include *mrck-1(ok586); let-502(fRNAi), mrck-1(ok586); ect-2(fRNAi), cdc-42(fRNAi); let-502(fRNAi), cdc-42(fRNAi); rho-1(fRNAi), cdc-42(fRNAi); ect-2(fRNAi), cgef-1(gk261); let-502(fRNAi), cgef-1(gk261); rho-1(fRNAi), and cgef-1(gk261); ect-2(fRNAi)*. All these double disrupted embryos exhibited defects in both Phase I and Phase II cortical myosin recruitment. *mrck-1(ok586)* embryos exhibited more severe phenotypes than did *mrck-1(fRNAi)* embryos. The images from Figure 6 are duplicated here for completeness. Scale bar is 10μm.

Movie 1: Time-lapse movie of GFP::GBDwsp-1 expressed in a *control(fRNAi)* embryo. Movie plays at 60x real time.

Movie 2: Time-lapse movie of GFP::GBDwsp-1 expressed in a *cdc-42(fRNAi)* embryo. Movie plays at 60x real time.

Movie 3: Time-lapse movie of GFP::GBDwsp-1 expressed in a *spd-5(fRNAi)* embryo. Movie plays at 60x real time.

Movie 4: Time-lapse movie of GFP::GBDwsp-1 expressed in a *par-2(fRNAi)* embryo. Movie plays at 60x real time.

Movie 5: Time-lapse movie of GFP::GBDwsp-1 expressed in a *par-6(zu222)* embryo. Movie plays at 60x real time.

Movie 6: Time-lapse movie of GFP::GBDwsp-1 expressed in an embryo coexpressing CDC-42(Q61L). Movie plays at 60x real time.

Movie 7: Time-lapse movie of GFP::GBDwsp-1 expressed in a *cgef-1(gk261)* embryo. Movie plays at 60x real time.

Movie 8: Time-lapse movie of GFP::GBDwsp-1 expressed in a *chin-1(tm1909)* embryo. Movie plays at 60x real time.

Movie 9: Time-lapse movie of GFP::PAR-6 expressed in a no-RNAi control embryo. Movie plays at 60x real time.

Movie 10: Time-lapse movie of GFP::PAR-6 expressed in a *cgef-1(gk261)* embryo. Movie plays at 60x real time.

Movie 11: Time-lapse movie of GFP::PAR-2 expressed in a no-RNAi control embryo. Movie plays at 60x real time.

Movie 12: Time-lapse movie of GFP::PAR-2 expressed in a *cgef-1(gk261)* embryo. Movie plays at 60x real time.

Movie 13: Time-lapse movie of GFP::CHIN-1 expressed in a no-RNAi control embryo. Movie plays at 60x real time.

Movie 14: Time-lapse movie of GFP::CHIN-1 expressed in a *cdc-42(fRNAi)* embryo. Movie plays at 60x real time.

Movie 15: Time-lapse movie of GFP::CHIN-1 expressed in a *par-6(fRNAi)* embryo. Movie plays at 60x real time.

Movie 16: Time-lapse movie of GFP::CHIN-1 expressed in a *par-2(fRNAi)* embryo. Movie plays at 60x real time.

Movie 17: Time-lapse movie of GFP::CHIN-1 expressed in a *par-1(fRNAi)* embryo. Movie plays at 60x real time.

Movie 18: Time-lapse movie of GFP::NMY-2 expressed in a no-RNAi control embryo. Movie plays at 60x real time.

Movie 19: Time-lapse movie of GFP::NMY-2 expressed in a *cgef-1(gk261)* embryo. Movie plays at 60x real time.

Movie 20: Time-lapse movie of GFP::NMY-2 expressed in a *cdc-42(fRNAi)* embryo. Movie plays at 60x real time.

Movie 21: Time-lapse movie of GFP::NMY-2 expressed in a *mrck-1(ok586)* embryo. Movie plays at 60x real time.

Movie 22: Time-lapse movie of GFP::NMY-2 expressed in an *ect-2(fRNAi)* embryo. Movie plays at 60x real time.

Movie 23: Time-lapse movie of GFP::NMY-2 expressed in a *rho-1(fRNAi)* embryo. Movie plays at 60x real time.

Movie 24: Time-lapse movie of GFP::NMY-2 expressed in a *let-502(fRNAi)* embryo. Movie plays at 60x real time.

Movie 25: Time-lapse movie of GFP::NMY-2 expressed in a *cdc-42(fRNAi); ect-2(fRNAi)* embryo. Movie plays at 60x real time.

Supplemental Movie 1: Time-lapse movie of GFP::CDC-42 expressed in a no-RNAi embryo. Movie plays at approximately 60x real time.

Supplemental Movie 2: Time-lapse movie of GFP::CGEF-1A expressed in a no-RNAi embryo. Movie plays at 60x real time.

Supplemental Table 1: Putative *C. elegans* Rho-family-directed GAP- and GEF-encoding genes screened for mislocalization of GFP::GBDwsp-1

Genes predicted to encode proteins with RhoGEF domains

Genetic Name	Molecular Name	RNAi Target	Screen Result	Notes
cgef-1 / tag-150	C14A11.3	both	+	HIT: RNAi embryos exhibit reduced loc at all phases
ect-2	T19E10.1	genomic	- other	ECT2 (mammalian RhoGEF) homolog; RNAi embryos are hypocontractile
tag-77	C28C12.10	genomic	-	
tag-52	C02F12.4	genomic	-	
rhgf-2	T08H4.1	genomic	-	RHo Guanine nucleotide exchange Factor
C11D9.1	C11D9.1	genomic	-	
uig-1	F32F2.1	genomic	-	Unc-112-Interacting Guanine nucleotide exchange factor
unc-73	F55C7.7	genomic	-	UNCoordinated
tag-218	K07D4.7	genomic	-	
Y105E8A.24	Y105E8A.24	cDNA	-	
unc-89	C09D1.1	genomic	-	UNCoordinated
exc-5	C33D9.1	genomic	-	EXCretory canal abnormal
R02F2.2	R02F2.2	genomic	-	
Y95B8A.12	Y95B8A.12	cDNA	-	
gei-18	Y37A1B.15	genomic	-	GEX Interacting protein
sos-1	T28F12.3	genomic	-	Drosophila SOS homolog
rhgf-1	F13E6.6	cDNA	-	RHo Guanine nucleotide exchange Factor
pix-1	K11E4.4	---	no result	PIX Interacting eXchange factor) homolog; no construct for RNAi

Genes predicted to encode proteins with RhoGAP domains

Gene Name	Molec Name	construct		Notes
chin-1 / BE0003N10.2	BE0003N10.2	cDNA	+	HIT: RNAi embryos exhibit abnormal PII and PIII probe loc
cyk-4	K08E3.6	genomic	- other	CYtoKinesis defect; RNAi embryos fail cytokinesis
rga-3	K09H11.3	genomic	- other	Rho GTPase Activating protein; RNAi embryos hypercontractile
rga-1	W02B12.8	genomic	-	Rho GTPase Activating protein

F23H11.4	F23H11.4	genomic	-	
ocrl-1	C16C2.3	genomic	-	OCRL (Lowe's oculocerebrorenal syndrome protein) homolog
srgp-1	F12F6.5	genomic	-	Slit-Robo GAP homolog
rga-2	Y53C10A.4	genomic	-	Rho GTPase Activating protein
hum-7	F56A6.2	genomic	-	Heavy chain, Unconventional Myosin
rlbp-1	T23G11.5	genomic	-	RaL Binding Protein
Y34B4A.8	Y34B4A.8	cDNA	-	
C01F4.2	C01F4.2	genomic	-	
gei-1	F45H7.2	genomic	-	
rga-4	Y75B7AL.4	cDNA	-	Rho GTPase Activating protein
T04C9.1	T04C9.1	genomic	-	
tag-341	ZK669.1	genomic	-	
2RSSE.1	2RSSE.1	cDNA	-	
pac-1	C04D8.1	genomic	-	PAR-6 At Contacts (abnormal early localization of PAR-6)
syd-1	F35D2.5	genomic	-	SYnapse Defective
tag-325	C38D4.5	genomic	-	
rrc-1	F47A4.3	genomic	-	RhoGAP for Rac-1 and Cdc-42
H08M01.2	H08M01.2	genomic	-	

Supplemental Table 2: Genetic interactions of *candidate GEF(RNAi)* with *cgef-1(gk261)*

	Brood size (N2)	Brood size (WH514)	Embryonic Survival (N2)	+/- SEM	Embryonic Survival (WH514)	+/- SEM	p-value for RNAi alone	p-value for interaction
none	211	226	99.6%	0.4%	98.8%	0.7%		
tag-52	274	175	99.6%	0.4%	89.7%	2.3%		
tag-127	236	170	100.0%	0.0%	67.0%	3.6%	*	*
C11D9.1	354	234	99.7%	0.3%	86.3%	2.2%		0.015
uig-1	211	307	100.0%	0.0%	98.0%	0.8%	*	*
unc-73	227	270	99.6%	0.4%	96.7%	1.1%		
tag-218	311	235	99.0%	0.6%	98.3%	0.8%		
Y105E8A.24	185	200	98.9%	0.8%	91.5%	2.0%		
unc-89	240	257	99.2%	0.6%	98.8%	0.7%		
exc-5	262	255	98.5%	0.8%	99.2%	0.6%	0.048	
R02F2.2	93	164	95.7%	2.1%	66.4%	3.7%	0.001	
Y95B8A.12	247	222	98.4%	0.8%	87.8%	2.2%	0.040	
gei-18	315	171	98.4%	0.7%	96.5%	1.4%	0.032	
sos-1	319	237	97.5%	0.9%	96.6%	1.2%	0.002	
rhgf-1	265	253	97.4%	1.0%	99.2%	0.6%	0.002	0.014
tag-77	326	181	98.2%	0.7%	94.5%	1.7%	0.014	

Brood size and embryonic survival from N2[*wild-type*] or WH514[*cgef-1(gk261)*] animals either untreated or treated with fRNAi directed at the indicated gene. Effects on embryonic survival of the depletion condition and of the interaction of the depletion condition with the *cgef-1(gk261)* genotype were investigated by logistic regression analysis. If statistically significant, the p-values of either parameter are presented above. Asterisks indicate that the p-value is uninformative due to the absence of observed dead embryos in the depletions of wild-type embryos of those conditions. Each tested condition was represented by at least two worms.

Supplemental Figure 1

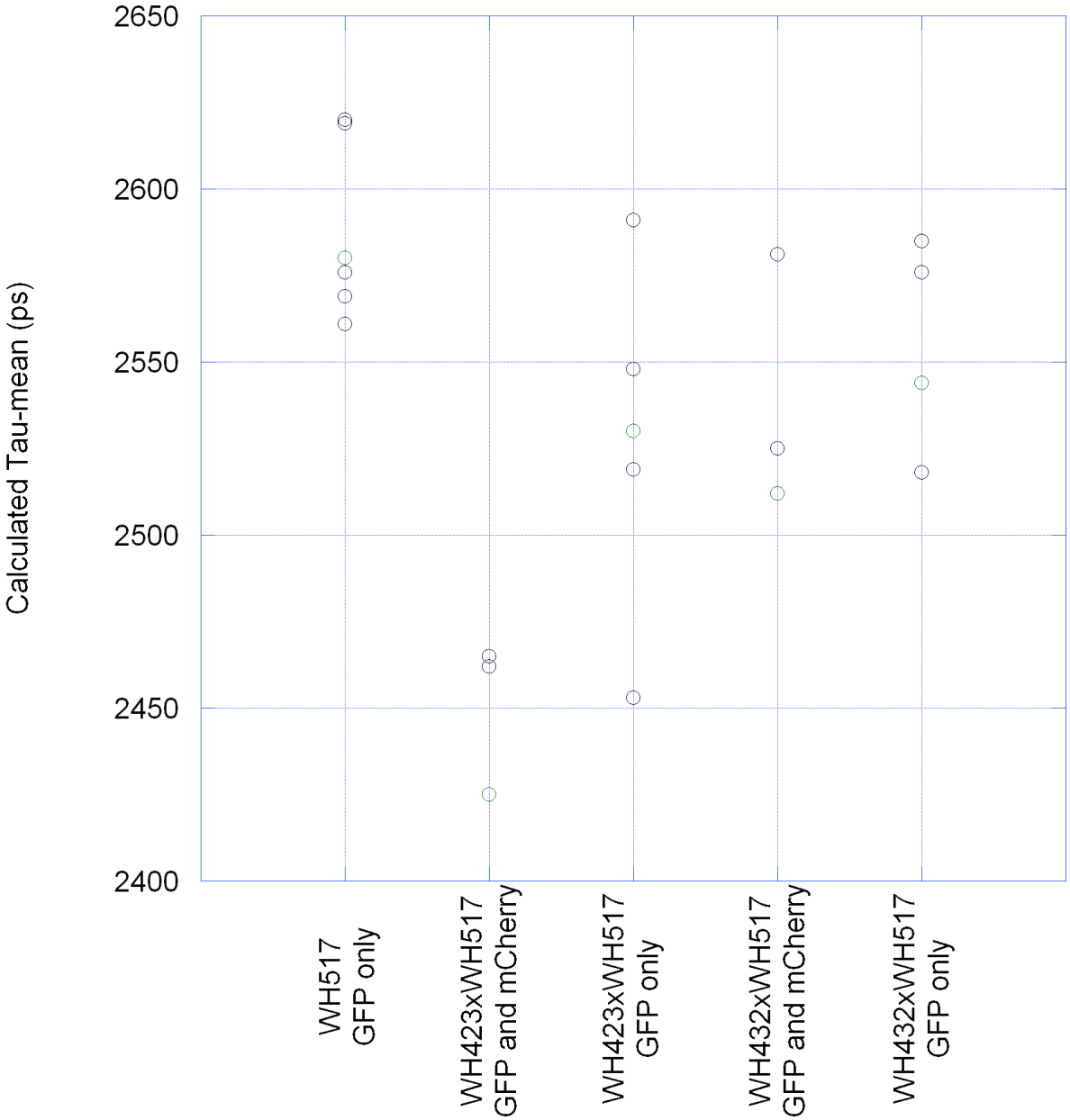

Supplemental Figure 2

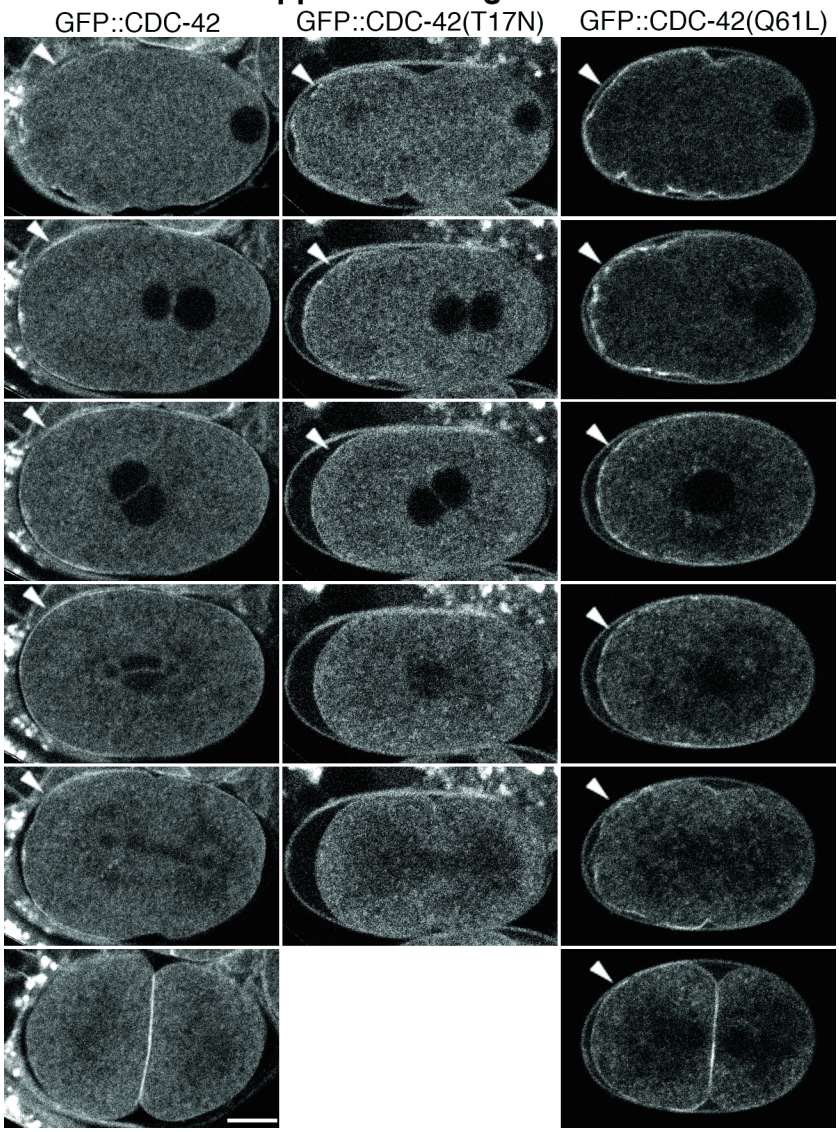

Supplemental Figure 3

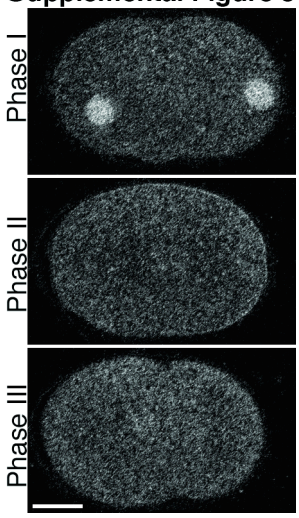

Supplemental Figure 4

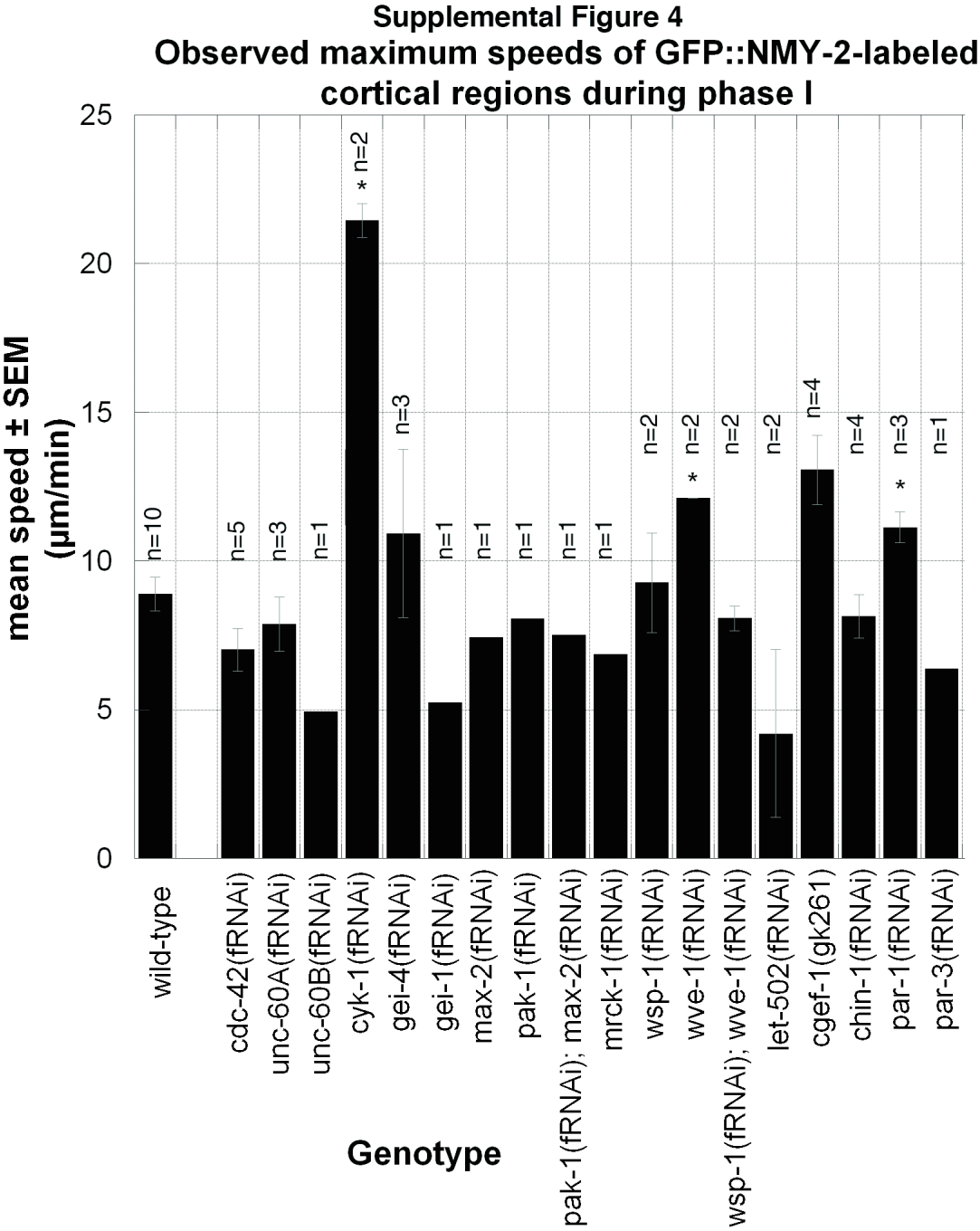

Supplemental Figure 5